Journal Name

ARTICLE

pH-induced transformation of ligated Au_{25} to brighter Au_{23} nanoclusters

Received 00th January 20xx,
Accepted 00th January 20xx

DOI: 10.1039/x0xx00000x

www.rsc.org/

Magdalena Waszkielewicz[a], Joanna Olesiak-Banska[a*], Clothilde Comby-Zerbino[b], Franck Bertorelle[b], Xavier Dagany[b], Ashu K. Bansal[c], Muhammad T.Sajjad[c], Ifor D.W. Samuel[c], Zeljka Sanader[f], Miroslawa Rozycka[d], Magdalena Wojtas[d], Katarzyna Matczyszyn[a], Vlasta Bonacic-Koutecky[e,g], Rodolphe Antoine[b], Andrzej Ozyhar[d], Marek Samoc[a]

Thiolate-protected gold nanoclusters have recently attracted considerable attention due to their size-dependent luminescence characterized by a long lifetime and large Stokes shift. However, the optimization of nanocluster properties such as the luminescence quantum yield is still a challenge. We report here transformation of $Au_{25}Capt_{18}$ (Capt labels captopril) nanoclusters occurring at low pH and yielding a product with much increased luminescence quantum yield which we have identified as $Au_{23}Capt_{17}$. We applied a simple method of treatment with HCl to accomplish this transformation and we characterized the absorption and emission of the newly-created nanoclusters as well as their morphology. Based on DFT calculations we show which Au nanocluster size transformations can lead to the highly luminescent species such as $Au_{23}Capt_{17}$.

Introduction

A new class of metallic nanomaterials containing thiolated gold nanoclusters (Au NCs) has been found to exhibit attractive physical and chemical properties.[1-7] Au NCs, containing a few up to several hundreds of gold atoms in the core surrounded by various ligands exhibit size-dependent luminescence, in the visible and/or NIR range of wavelengths .[8, 9] The presence of emission in the NIR (in the biological transparency window region) is essential for applications of gold nanoclusters in biology and medicine. As most of biomolecules have low absorption coefficients in this range, a risk of irritation of normal metabolism is limited and the autofluorescence of the biological material is minimized as well as deep penetration (>1 cm) of the tissue is possible.[10] Although strategies based on silver doping[11] or rigidifying the ligand shell have been proposed to enhance the photoluminescence quantum yield of the clusters both in the linear[12] and nonlinear optical regime[13], it is usually rather low, and has been found to be strongly cluster size dependent.[8] The ligands may play an important role in fluorescence enhancement,[14] and both the ligands and the nanocluster size may determine the activity and biodistribution in context of applications *in vivo*. Therefore, a precise choice of the stabilizing ligands is required, as well as the control of the quantum cluster size with the "atomic precision".

Major synthetic breakthroughs have been achieved using two systematic approaches: size-focusing methodology[15] and ligand exchange-induced size/structure transformation (LEIST) methodology.[16] However, a transformation consisting in removing one or two metal atoms and/or ligands from a stable nanocluster size remains challenging. Core etching[17] or using reductive conditions[18] have permitted size conversion of AuNCs from Au_{25} to Au_{22} and Au_{23}. Recently, an elegant strategy using a two-step metal exchange method has allowed for the "resection" of two surface gold atoms leading to the transformation from Au_{23} to Au_{21} NCs[19]. Another size-controlled synthesis of aqueous nanoclusters can be obtained through pH control. Xie and co-workers achieved a size-tunable synthesis of $Au_{10–12}$, Au_{15}, Au_{18}, and Au_{25} nanoclusters, under pH adjustment utilizing carbon monoxide (CO) as a mild reducing agent.[20]

In this contribution, we report making of highly fluorescent NCs by size transformation of well-characterized Au_{25} stabilized by

[a.] *Advanced Materials Engineering and Modelling Group, Faculty of Chemistry, Wroclaw University of Science and Technology, Wybrzeze Wyspianskiego 27, 50-370 Wroclaw, Poland*
[b.] *Univ Lyon, Université Claude Bernard Lyon 1, CNRS, Institut Lumière Matière, UMR 5306 F-69622, Lyon, France*
[c.] *Organic Semiconductor Centre, SUPA, School of Physics and Astronomy, University of St. Andrews, St. Andrews, KY16 9SS, United Kingdom*
[d.] *Department of Biochemistry, Wroclaw University of Science and Technology, Wybrzeze Wyspianskiego 27, 50-370 Wroclaw, Poland*
* e-mail: joanna.olesiak-banska@pwr.edu.pl
e. Center of Excellence for Science and Technology-Integration of Mediterranean region (STIM) at Interdisciplinary Center for Advanced Sciences and Technology (ICAST), University of Split, Meštrovićevo šetalište 45, HR-21000 Split, Republic of Croatia
f. Faculty of Science, University of Split, *Rudera Boskovica 33*, HR-21000 Split, Republic of Croatia
g. Department of Chemistry, Humboldt Universitat zu Berlin, Brook-Taylor-Strasse 2, 12489 Berlin, Germany.
Electronic Supplementary Information (ESI) available: TEM images of nanoclusters, absorption and photoluminescence spectra, electrophoresis details. See DOI: 10.1039/x0xx00000x

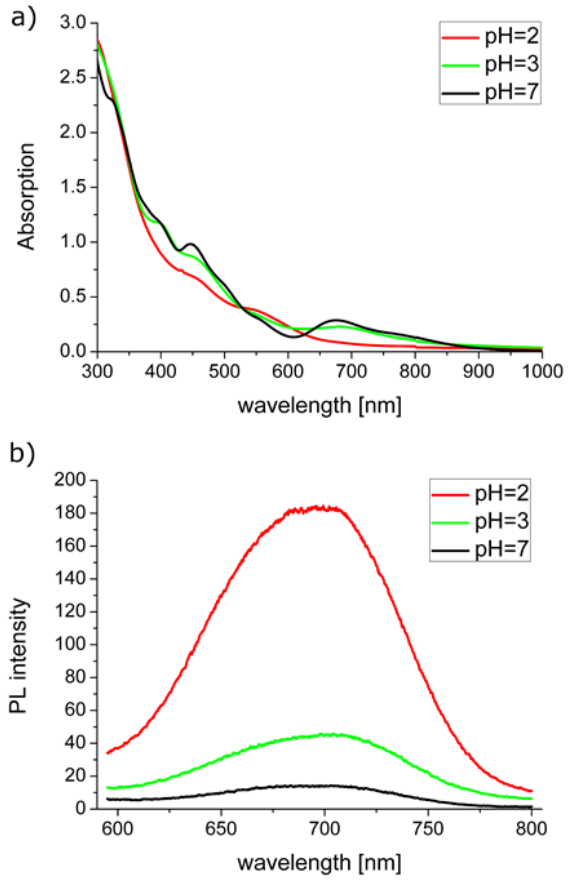

Figure 1. Absorption (a) and emission (b) spectra of AuCapt measured after several hours of incubation in buffers of various pH. The samples were excited with 550 nm.

captopril (Capt) ligand occurring on treatment with low pH. The transformation of Au_{25} NCs into Au_{23} NCs is confirmed by electrospray ionization mass spectrometry and qualitative theoretical explanation based on DFT calculations.

Results

The captopril protected gold (AuCapt) nanoclusters were synthesized according to a literature procedure[21] and dispersed in water (pH=7). They exhibited absorption bands at 800, 675, 550, 505, 445and 400 nm (Fig.1a), similar to the $Au_{25}(PET)_{18}$ (where PET – phenylethanethiol) clusters reported by Jin and co-workers.[22] After transferring the nanoclusters to buffers with pH ranging from 2 to 10, no change has been initially observed in the absorption spectra. However, after several hours the absorption spectra for NCs in pH=2 lost the features characteristic of Au_{25} NCs i.e. absorption bands at 800, 670 nm and 450 nm gradually decreased. Additionally, a small shoulder at 550 nm developed into a band (Fig.1a). For pH=3 the leading features of the absorption spectrum were also partly lost, but for other pH values (between 4 to 10) no changes occurred (see SI Fig.S1).

The photoluminescence (PL) spectra measured upon treatment with low pH revealed enhancement in the nanoclusters emission with a maximum at 700 nm (when excited at 550 nm, corresponding to Stokes shift of 0.12 eV).

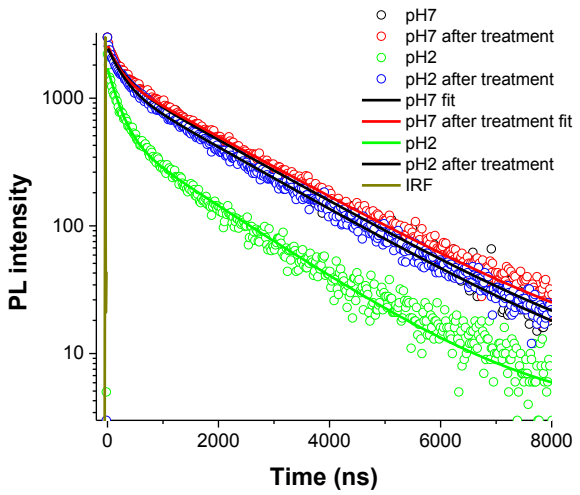

Figure 2. PL decays of AuCapt in pH = 7 (black), AuCapt in pH = 2 (green) and nanoclusters after treatment (drying and redissolving in pH = 7 buffer): AuCapt pH = 7 after treatment (red) and AuCapt pH = 2 after treatment (blue). IRF – instrument response function.

In order to compare the PL intensities, the data were normalized with respect to the same absorbance at the excitation wavelength. The PL intensity of NCs at pH = 2 was found to be an order of magnitude higher than that reported for nanoclusters at pH = 7 (Fig.1b). The PL quantum yield (QY) of the nanoclusters was calculated by comparing their emission with fluorescence of a standard which was Oxazine 170.[23] AuCapt NCs at pH= 7 have QY = 0.37% whereas at pH = 2 the QY increased ~10 times, up to 3.9%.

This dramatic increase of the brightness of the nanoclusters needs therefore to be understood in terms of the possible structural changes. One of the possibilities considered was the formation of Au(I)-Capt which is an intermediate in the synthesis of $Au_{25}Capt_{18}$. Since Au(I) complexes are known to fluoresce[24], it might be assumed that the observed emission enhancement is connected with the presence of a significant amount of this Au(I)-Capt polymer. To investigate the potential impact of the polymer on emission of the NC solution at pH=2, we recorded separately its emission spectrum. The fluorescence was observed in the range between 400 and 660 nm with the maximum at 465 nm, which does not provide explanation of the emission enhancement of the nanoclusters (see SI Fig.S2).

To clarify if the observed changes arise due the presence of protonation or to chloride ions in the buffer solution, the neutral and concentrated solution of AuCapt was dissolved in HCl and HNO_3, both corresponding to pH = 2. The samples emission and absorption were monitored over 24 hours, as well as after 72 hours. The comparison of the absorption and emission spectra is presented in Figs. S3-S4, which show that a restructuration of the spectra has occurred. The process was identical in the case of samples with the pH = 2 buffer and with HCl, and was completed in 5 hours. In contrast, in the sample with HNO_3, different features are observed (SI Fig. S3).

The luminescence decays were measured and fitted with double exponential function (Fig. 2). The PL lifetimes were found to depend only slightly on the pH, in case of the sample in pH = 7, they were τ_1 = 264 (0.09) and τ_2 = 1778 ns (0.91) with the average 1753 ns. For the sample in pH = 2, τ_1 = 207 (0.18) and τ_2 = 1516 ns (0.82), giving average of 1462 ns. The corresponding lifetime values are presented in Table 1.

Table 1. PL lifetimes and QY of AuCapt in pH = 7 and 2 and after treatment (drying and redissolving in pH=7 buffer).

AuCapt	pH=7 (QY = 0.37%)	pH=7 after treatment	pH=2 (QY = 3.9%)	pH=2 after treatment
τ_1 [ns]	264 (0.09)	200 (0.08)	207 (0.18)	250 (0.12)
τ_2 [ns]	1778 (0.91)	1809 (0.92)	1516 (0.82)	1757 (0.88)
<τ> [ns]#	1753	1794	1462	1728

average lifetime $\langle\tau\rangle = (a_1\tau_1^2+a_2\tau_2^2)/(a_1\tau_1+a_2\tau_2)$

In order to test the reversibility of changes induced by low pH, we dried and redissolved the samples in a buffer of pH = 7. In the case of AuCapt at pH = 2, the absorption and emission spectra were preserved (SI Fig.S5). However, an increase of the PL lifetime was observed, and the value of the long component changed from ~1500 ns to ~1750 ns, which is a value similar to the lifetime of AuNC at pH = 7 (see Fig.2). For AuCapt at pH = 7 the lifetimes did not change after drying and redissolving the sample.

Since the absorption of NCs at pH=2 did not unambiguously correspond to any reported absorption spectrum in the literature[25], we checked whether we obtained a mixture of the products. For this reason the polyacrylamide gel electrophoresis (PAGE) was conducted and two separated bands were observed (see Fig. 3a). In order to identify the responsible species, the ESI-MS was carried out for the desalted product mixture as well as for AuCapt before the low pH treatment (Fig. 3b and c, and Fig. S6). The corresponding ESI deconvolution spectrum leads to $Au_{25}Capt_{18}$ before and after the low pH treatment leads to several peaks with smaller masses, which correspond to a mixture of $Au_{24}Capt_{16}$and $Au_{23}Capt_{16}$ and $Au_{23}Capt_{17}$ and $Au_{22}Capt_{17}$.

The separated NCs, extracted from a gel, were characterized by UV/Vis spectroscopy (Fig. S7). The absorption spectrum of upper fraction presents two bands at 460 and 575 nm. Similarly, the band of lower fraction was located at 575 nm with a shoulder at 460 nm. The emission spectra of separated fractions were blue-shifted by 6 nm with respect to the one for NCs in pH=2. However, more important findings are that the lower fraction has much higher luminescence quantum yield equal to ~5 % , when compared to the upper fraction which is ~0.1 %.

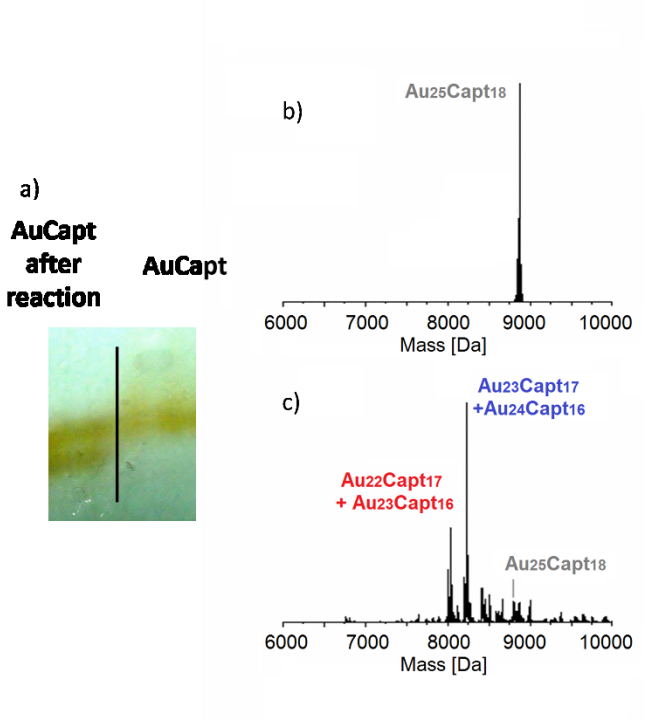

Figure 3. a) Polyacrylamide gel electrophoresis of the product allowed to obtain two bands (left side), where the upper one is very similar to the basic sample Au25 (right side). ESI-MS analysis showed a detailed composition of the product. Well defined Au25Capt18 was used as control. Deconvoluted deconvoluted ESI-MS spectrum of AuCapt NCs before (b) and after pH=2 treatment (c). The corresponding ESI-MS spectra are given in Fig. S6 in SI.

Discussion

In our experiments, the originally synthesized nanoclusters exhibited the absorption spectra with all the bands characteristic for $Au_{25}(SR)_{18}$. Based on the absorption spectra and ESI-MS results, we can confirm the formation of $Au_{25}(Capt)_{18}$ nanoclusters, with no need for post-synthesis separation.

Au25 PL decay times reported in the literature depend on the emission wavelength and stabilizing ligands. Link et al. reported biexponential decays for AuSG NCs, with lifetime values ranging from 177 ns/1380 ns for emission at 700 nm to 341 ns/1480 ns for emission at 800 nm.[26] Wu et al. obtained single PL lifetimes of about 500-700ns for Au25 with $-SC_2H_4Ph$, $-SC_{12}H_{25}$, and $-SC_6H_{13}$ ligands as well as two PL lifetimes of 247 ns/1240 ns for $Au_{25}SG_{18}$ NCs.[27]These data are in a good agreement with our results of PL decays. AuCapt functionalized clusters presented lifetimes of 210 ns/1790 ns (table 1), similar to those for other ligands with electron-rich groups.

It has been shown in some reports that gold nanoclusters exhibit good stability under pH although results on the influence of pH on PL intensity evolution differ considerably [28, 29,30] Our work shows that after an incubation with HCl (pH = 2), the nanoclusters transform into species with increased luminescence. Based on the MS analysis and on the agreement

between experimental and theoretical absorption spectra for $Au_{23}L_{17}$ (see Fig. 4), we recognized the transformation as being from $Au_{25}(SR)_{18}$ to $Au_{23}Capt_{17}$ (Au23). The proposed composition of $Au_{23}SR_{17}$ was reported in the literature as possibly emitting bright red PL.[31]

In this contribution, we show that application of low pH in the presence of Cl^- ions is a new method of transformation from one stable size of nanoclusters to another, with the nanoclusters being produced with the same ligand, in water. On the contrary, previous protocols required thermal treatment and high excess of the thiol that substitute the outgoing ligand.[16] Moreover, the incoming ligand was required to be significantly different from the original one. In early work simple ions like Cl^- or OH^- were used to stabilize the nanoclusters, but they exhibited low stability in drying process. Other studies showed the charge conversion of $[Au_{25}(SCH_2CH_2Ph)_{18}]^0$ clusters into anionic form in the presence of halide ions.[32] In our studies comparison of HCl and HNO_3 treatment shows that the presence of Cl^- ions is important for the size transformation. On the other hand, application of nitric acid leads to the protonation of clusters. Relative intensities of 800 nm/630 nm and 450 nm/400 nm absorption peaks might be connected with the change of the charge of ligated Au_{25} nanoclusters. High intensity of 800 nm and 450 nm peaks, as observed in our samples before treatment, is characteristic for anionic clusters.[33] After HNO_3 treatment the changes in absorption spectra shown in Fig.S3a are characteristic for the neutral cluster $[Au_{25}SR_{18}]^0$.[33] A similar absorption spectrum is observed at pH=3 with HCl.

Thus, one can suggest that the acidic treatment leads to at least two-step transformation process: (1) pH=3, conversion process of the $[Au_{25}SR_{18}]^-$ anionic cluster into a charge neutral cluster $[Au_{25}(SR)_{18}]^0$ and (2) pH=2, degradation of the NCs with a loss of Au_2SR or Au_3SR, leading to fluorescent $Au_{23}(SR)_{17}$ and other sizes.

The first stage could be explained on the basis of the pK_a value for carboxylic group of captopril, which is equal to 3.35 ± 0.04 (for the structure of ligand see Fig. S9)[34]. The protonation of NCs occurs in pH ~ 3 and lower.

The degradation of NCs in the presence of halides was reported before by Zu et al.[32] In that case two types of salts were used – NaX and TOAX (where X – halide), but only NaX caused decomposition. Also in our work chloride ions played crucial role in the second stage of the transformation process. Although $Au_{25}(Capt)_{18}$ were stabilized with TOA^+ during whole process, the dramatically low pH could shift the equilibrium in our system. In pH = 2, TOA^+ had limited stabilizing activity on protonated NCs and as a result partial decomposition of nanoparticles with Cl^- anions was possible. A Cl^- ion, due to its higher electronegativity, acts as an acceptor of electrons and, when in contact with Au surface, electronic charge transfer from gold ions to chloride ions occurs. Additionally, the protonation of carboxylic groups decreases the electron density in the outer layer of NCs and thus chloride - gold interactions become more prominent. On the other hand, NO_3^- has never

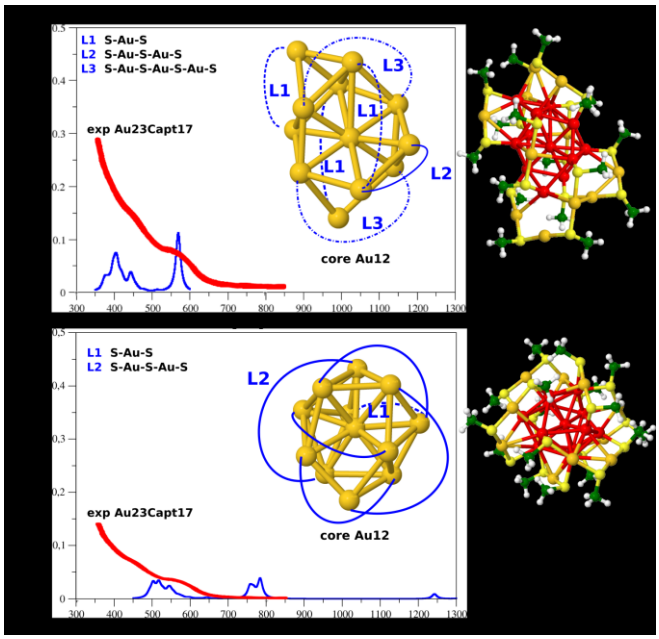

Figure 4. Comparison between experimental (red line) and TDDFT calculated apsorption spectra (blue lines) for a) lowest energy structure of $Au_{23}Capt_{17}$ obtained by adding one ligand to $Au_{23}Capt_{16}$ and b) for higher energy structure (by 0.5eV) of $Au_{23}Capt_{17}$ obtained by removing two Au atoms and one ligand from $Au_{25}Capt_{18}$. Captopril ligands are replaced by $-SCH_3$ groups in the calculations, for DFT calculations pbe0 functional and def2svp AO basis have been used.

been reported as decomposition agent, but is known as a strong oxidant, which supports the change of oxidation state of NCs. The mechanism of size transformation is schematically shown in Scheme 1.

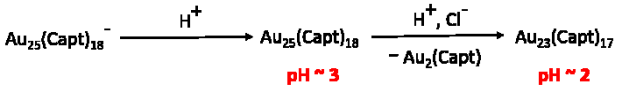

Scheme 1. Suggested Au25 → Au23 transformation mechanism. The process is two-stage: in the first anionic Au25 is oxidized to the neutral form, in the second step partial degradation appears with loss of $Au_2(Capt)$.

One notes that the pH-induced transformation described here, has some similarity with the recently reported results from Jin et al. where $[Au_{25}(SePh)_{18}]^-$ nanoclusters were transformed into the $[Au_{23}(SePh)_{16}]^-$ nanocluster in the presence of $NaBH_4$.[18] In fact our computational results show that the transformation from $Au_{23}L_{16}$ to $Au_{23}L_{17}$ is more favorable than from $Au_{25}L_{18}$ to $Au_{23}L_{17}$. In the former case, addition of ligand to $Au_{23}L_{16}$ which is also stable produces the most stable $Au_{23}L_{17}$ with structure containing core of 12 Au atoms as shown in Fig. 4a), for which the calculated absorption spectrum is in a good agreement with experimental findings. In contrast, the structure of $Au_{23}L_{17}$ derived from $Au_{25}L_{18}$ by removing two gold atoms and one ligand is higher in energy and the TDDFT calculated absorption spectrum is not in agreement with experimental findings as shown in Fig. 4b). Although the core contains 12 atoms, its structure is different with respect to the one obtained starting from $Au_{23}L_{16}$. Since the excitation within the core is responsible for absorption spectra, its structural properties are responsible

for the leading features. The above results show that the removal of the gold atoms and ligand versus addition of a ligand cause a reconstruction of the core which is responsible for the optical properties including fluorescence.

Conclusions

We presented here a new approach to transform Au nanoclusters of one size into another. In our simple method a low pH treatment (with HCl) was successfully applied for the nanoclusters transformation from $Au_{25}Capt_{18}$ to very fluorescent $Au_{23}Capt_{17}$. We monitored the changes of nanocluster absorption and emission spectra in the course of the transformation and measured the fluorescence decay times of the substrates and products. We observed enhancement of the fluorescence by up to 13 times when the nanocluster size changed. In fact, changes of optical properties by changing number of Au atoms and ligands occur due to structural changes, as shown by our theoretical findings. The final nanoclusters were stable after the transition from low to neutral pH. Because Au_{25} are the most easily obtained nanoclusters, our findings about their pH sensitivity and size transformation with corresponding fluorescence enhancement provide significant information useful for their further applications. Moreover, our approach gives a relatively simple procedure for the preparation of highly fluorescent Au_{23} nanoclusters from Au_{25}. It may also be possible to obtain other sizes by using other monodispersed nanoclusters as a substrate.

Experimental

Chemicals. All of the chemicals were commercially available and used without further purification. Gold(III) chloride trihydrate ($HAuCl_4 \cdot 3H_2O$, 99.999%), captopril (Capt, 98%), sodium borohydride ($NaBH_4$, 98%) and tetraoctylammonium bromide (TOABr, 98%) were purchased from Sigma-Aldrich. Aqueous 40% acrylamide and bisacrylamide stock solution (37.5:1), N,N,N',N'-tetramethylethylenediamine (TEMED, 99%), N,N'-methylene bisacrylamide (Bis, >98%) and 10x concentrated SDS-PAGE running buffer (SDS) were supplied from Carl Roth. Ammonium persulfate (APS, 98%), 0.5 M Tris-HCl buffer pH 6.8, and 1.5M Tris-HCl buffer pH 8.8 were purchased from BIO-RAD.The universal buffer solutions (pH 2 - 10) were supplied from Avantor Performance Materials Poland. The deionized water with the resistivity of 18 MΩ·cm was used in the studies.

Instrumentation and protocols. High-resolution transmission electron microscopy (TEM) was conducted with a FEI Tecnai G2 20 X-TWIN. TEM images of AuCapt nanoclusters in pH = 2, 3 and 7 are presented in Fig. S8 in SI. The absorption and fluorescence measurements were recorded on a JASCO V-670 spectrophotometer and a Hitachi F-4500 spectrofluorometer, respectively. Excited state lifetimes were measured with an Edinburgh Instruments FLS980 Fluorescence Spectrometer. All samples were excited at 379 nm with a PicoQuant pulsed laser and emission was detected at 720 nm using time-correlated single-photon counting (TCSPC). The experimental data was fitted with two exponential decays.

Evolution of the gold NC size without and with acid treatment was determined by electrospray ionization on a commercial quadrupole time-of-flight (micro-qTOF, Bruker-Daltonics, Bremen, Germany, mass resolution 10 000). AuCapt NCs without acid treatment and the same sample after the treatment (HCl, pH = 2) were prepared to a final concentration approximately of 50μM in water. The samples were analysed in negative ion mode: each data point was the summation of spectra over 5 min. External calibration was carried out with a set of synthetic peptides. We used our $Au_{25}Capt_{18}$ NCs to optimize the mass spectrometer and define the measurement uncertainties. Due to the huge amount of sodium adducts observed in ESI-MS, we decided to perform desalting procedure before MS analysis. The AuNC was dissolved in 1mL of methanol (or water). Then 1mL of glacial acetic acid was added and precipitation was induced by adding THF. Then the sample was centrifuged and dried.

A multiplicative correlation algorithm (MCA) was used to estimate the mass of nanoparticles from the mass-to-charge spectra produced by electrospray ionization mass spectrometry.[35, 36]

Preparation of AuCapt Clusters. Captopril-protected Au_{25} clusters were prepared using a modified Kumar one-pot procedure.[21] Briefly, TOABr (0.23 mmol, 126.8 mg) was dissolved in 10 mL of methanolic solution of $HAuCl_4 \cdot 3H_2O$ (0.02 M) and stirred vigorously. After 20 min, 1 mmol of captopril (217.2 mg) was dissolved in 5 mL of methanol and rapidly added into the reaction mixture under stirring. After 30 min, 5 mL of aqueous solution of $NaBH_4$ (0.4 M), cooled to 4°C, was rapidly poured to the reaction mixture under vigorous stirring. The solution was allowed to react for 8 h in an ice bath. The suspension was centrifuged to remove unreacted, insoluble Au(I):SR polymers. The supernatant was collected and concentrated in water bath at 45°C. The clusters were precipitated with ethanol and repeatedly washed with methanol and ethanol. The final precipitate was dried in 45°C.

Polyacrylamide Gel Electrophoresis (PAGE) The electrophoresis in a discontinuous gel system was carried out by using a PROTEAN II XL Cell slab gel electrophoresis unit (BIO-RAD). The separating and stacking gels were prepared from acrylamide monomers with the final concentrations of 18.3 %T; 4.2 %C (separating) and 7.5 %T; 2.6 %C (stacking), where %T – total monomer (acrylamide + bisacrylamide) concentration and %C – concentration of the cross-linking. The clusters were dissolved in a 5% (v/v) glycerol/water solution. The electrophoresis was carried out for 13 h at a constant voltage mode (150 V) at 4°C. Finally, the separating gel was cut into bands and the particular fractions were eluted with water.

Theoretical

Density functional theory (DFT) has been used to determine the properties of the liganded gold structures employing the SVP atomic orbital basis set for all atoms [37] and the relativistic effective core potential (RECP) of the Stuttgart group for gold atoms. [38]

The search for structures was performed using simulated annealing simulations as implemented in Turbomole quantum chemistry program. [39] Coordinates for starting structures were taken from crystal structures of $Au_{23}L_{16}^{-}$ [40] and $Au_{25}L_{18}$ [41] where different ligands were replaced by SCH_3.

The found structures were subsequently reoptimized using PBE functional. [42, 43] The absorption spectra were computed using Perdew–Burke–Ernzerhof exchange–correlation functional (PBE0). [43]

Contributions

JOB conceived the initial idea and coordinated the work, MWa prepared the nanoparticles, MWa and JOB measured optical properties, MWa, JOB, MS analyzed the results. CCZ, FB, XD, RA performed and analyzed ESI-MS experiments. AKB, MTS, IDWS performed and analyzed PL lifetime measurements. ZS, VBK performed and analyzed DFT simulations. MR, MWa, MWo performed PAGE separation experiments. MS, RA, VBK, KM, IDWS, AO supervised and financed the project. JOB, MWa, RA, VBK wrote the paper. All the authors provided critical feedback and helped to shape the final manuscript.

Acknowledgements

This work was supported by the National Science Centre under grants DEC-2013/10/A/ST4/00114 and DEC-2013/09/B/ST5/03417 and by a statutory activity subsidy from the Polish Ministry of Science and Higher Education for the Faculty of Chemistry of Wroclaw University of Science and Technology. We would like to acknowledge financial support of the French-Croatian project. “International Laboratory for Nano Clusters and Biological Aging, LIA NCBA. IDWS acknowledges support from a Royal Society Wolfson Research Merit Award. This research was supported by STIM - REI, a project funded by European Union from European Structural and Investment Funds 2014. - 2020., Contract Number KK.01.1.1.01.0003.

Notes and references

1. S. Knoppe and T. Burgi, *Accounts Chem Res*, 2014, **47**, 1318-1326.
2. Y. Z. Lu and W. Chen, *Chem Soc Rev*, 2012, **41**, 3594-3623.
3. C. Noguez and I. L. Garzon, *Chem Soc Rev*, 2009, **38**, 757-771.
4. N. Sakai and T. Tatsuma, *Adv Mater*, 2010, **22**, 3185-3188.
5. M. Z. Zhu, C. M. Aikens, M. P. Hendrich, R. Gupta, H. F. Qian, G. C. Schatz and R. C. Jin, *J Am Chem Soc*, 2009, **131**, 2490-2492.
6. J. Olesiak-Banska, M. Waszkielewicz, K. Matczyszyn and M. Samoc, *RSC Advances*, 2016, **6**, 98748-98752.
7. R. Antoine, Bonačić-Koutecký, Vlasta, *Liganded silver and gold quantum clusters. Towards a new class of nonlinear optical nanomaterials*, Springer International Publishing, 2018.
8. L.-Y. Chen, C.-W. Wang, Z. Yuan and H.-T. Chang, *Analytical Chemistry*, 2015, **87**, 216-229.
9. X. Qu, Y. Li, L. Li, Y. Wang, J. Liang and J. Liang, *Journal of Nanomaterials*, 2015, **2015**, 23.
10. I. Martinić, S. V. Eliseeva and S. Petoud, *Journal of Luminescence*, 2017, **189**, 19-43.
11. X. Guevel, C. Spies, N. Daum, G. Jung and M. Schneider, *Nano Res.*, 2012, **5**, 379-387.
12. K. Pyo, V. D. Thanthirige, K. Kwak, P. Pandurangan, G. Ramakrishna and D. Lee, *Journal of the American Chemical Society*, 2015, **137**, 8244-8250.
13. F. Bertorelle, C. Moulin, A. Soleilhac, C. Comby-Zerbino, P. Dugourd, I. Russier-Antoine, P.-F. Brevet and R. Antoine, *ChemPhysChem*, 2018, **19**, 165-168.
14. Z. K. Wu and R. C. Jin, *Nano Lett.*, 2010, **10**, 2568-2573.
15. R. Jin, H. Qian, Z. Wu, Y. Zhu, M. Zhu, A. Mohanty and N. Garg, *The Journal of Physical Chemistry Letters*, 2010, **1**, 2903-2910.
16. C. Zeng, Y. Chen, A. Das and R. Jin, *The Journal of Physical Chemistry Letters*, 2015, **6**, 2976-2986.
17. M. A. H. Muhammed, P. K. Verma, S. K. Pal, R. C. A. Kumar, S. Paul, R. V. Omkumar and T. Pradeep, *Chemistry – A European Journal*, 2009, **15**, 10110-10120.
18. Y. Song, H. Abroshan, J. Chai, X. Kang, H. J. Kim, M. Zhu and R. Jin, *Chemistry of Materials*, 2017, **29**, 3055-3061.
19. Q. Li, T.-Y. Luo, M. G. Taylor, S. Wang, X. Zhu, Y. Song, G. Mpourmpakis, N. L. Rosi and R. Jin, *Science Advances*, 2017, **3**.
20. Y. Yu, X. Chen, Q. Yao, Y. Yu, N. Yan and J. Xie, *Chemistry of Materials*, 2013, **25**, 946-952.
21. S. Kumar and R. Jin, *Nanoscale*, 2012, **4**, 4222-4227.
22. M. Zhu, C. M. Aikens, F. J. Hollander, G. C. Schatz and R. Jin, *J. Am. Chem. Soc.*, 2008, **130**, 5883-5885.

23. K. Rurack and M. Spieles, *Anal Chem*, 2011, **83**, 1232-1242.
24. A. Vogler and H. Kunkely, *Coordination Chemistry Reviews*, 2001, **219-221**, 489-507.
25. C. J. Zeng, Y. X. Chen, A. Das and R. C. Jin, *J Phys Chem Lett*, 2015, **6**, 2976-2986.
26. S. Link, A. Beeby, S. FitzGerald, M. A. El-Sayed, T. G. Schaaff and R. L. Whetten, *J Phys Chem B*, 2002, **106**, 3410-3415.
27. Z. K. Wu and R. C. Jin, *Nano Lett*, 2010, **10**, 2568-2573.
28. X. L. Guevel, O. Tagit, C. E. Rodriguez, V. Trouillet, M. Pernia Leal and N. Hildebrandt, *Nanoscale*, 2014, **6**, 8091-8099.
29. Y. Yu, Z. T. Luo, D. M. Chevrier, D. T. Leong, P. Zhang, D. E. Jiang and J. P. Xie, *J Am Chem Soc*, 2014, **136**, 1246-1249.
30. T. Huang and R. W. Murray, *J Phys Chem B*, 2001, **105**, 12498-12502.
31. R. Hamouda, F. Bertorelle, D. Rayane, R. Antoine, M. Broyer and P. Dugourd, *International Journal of Mass Spectrometry*, 2013, **335**, 1-6.
32. M. Zhu, G. Chan, H. Qian and R. Jin, *Nanoscale*, 2011, **3**, 1703-1707.
33. M. Zhu, W. T. Eckenhoff, T. Pintauer and R. Jin, *The Journal of Physical Chemistry C*, 2008, **112**, 14221-14224.
34. M. R. Popović, G. V. Popović and D. D. Agbaba, *Journal of Chemical & Engineering Data*, 2013, **58**, 2567-2573.
35. D. Shen, M. Henry, V. Trouillet, C. Comby-Zerbino, F. Bertorelle, L. Sancey, R. Antoine, J.-L. Coll, V. Josserand and X. L. Guével, *APL Materials*, 2017, **5**, 053404.
36. C. Truillet, F. Lux, O. Tillement, P. Dugourd and R. Antoine, *Anal Chem*, 2013, **85**, 10440-10447.
37. F. Weigend and R. Ahlrichs, *Physical Chemistry Chemical Physics*, 2005, **7**, 3297-3305.
38. D. Andrae, U. Häußermann, M. Dolg, H. Stoll and H. Preuß, *Theoretica chimica acta*, 1990, **77**, 123-141.
39. *Journal*, 2016.
40. A. Das, T. Li, K. Nobusada, C. Zeng, N. L. Rosi and R. Jin, *J Am Chem Soc*, 2013, **135**, 18264-18267.
41. M. W. Heaven, A. Dass, P. S. White, K. M. Holt and R. W. Murray, *J Am Chem Soc*, 2008, **130**, 3754-3755.
42. J. P. Perdew and Y. Wang, *Physical Review B*, 1992, **45**, 13244-13249.
43. J. P. Perdew, K. Burke and M. Ernzerhof, *Phys Rev Lett*, 1996, **77**, 3865-3868.